Delocalization in Substituted Benzene Dications: A Magnetic Point of View

Mesías Orozco-Ic,[a] Jorge Barroso,[a] Rafael Islas,[b] and Gabriel Merino*[a]

In this work, the induced magnetic field is analyzed for a series of substituted benzenes dications with formula $C_6R_6^{2+}$ (R=I, At, SeH, $SeCH_3$, TeH, $TeCH_3$), presumably exhibiting concentric aromaticity. Previous studies concluded that in the carbon skeleton, just π-electrons are delocalized. However, our results support that both the σ- and π-electrons are delocalized in the carbon skeleton, combined with a σ-delocalization in the external ring. The role of the relativistic effects in these dications is discussed in detail.

1. Introduction

For almost 150 years, aromaticity has been used to explain exclusively the properties of benzene derivatives (or similar ring systems) as a consequence of the π-electrons delocalization in the ring,[1] but quite recently it has been extended to inorganic compounds.[2–6] In aromatic systems composed exclusively by metals, both σ- and π-electrons are delocalized (multiple aromaticity).[7–8] In 1988, Sagl and Martin synthesized a fascinating system with formula $C_6I_6^{2+}$, which is obtained through hexaiodobenzene oxidation.[9] The authors suggested that $C_6I_6^{2+}$ is a molecule with two concentric rings, one formed by the internal C_6-ring, and the other one by the outer iodine atoms.[9–11] The carbon ring is, in principle, π-delocalized, and the external iodine ring is concomitantly σ-delocalized, so it is an organic double aromatic system. Some derivatives of this dication were also explored as putative concentric and double aromatic species by Hatanaka and coworkers[12] via Nucleus Independent Chemical Shift (NICS) computations.[13–15] They found that both rings in $C_6I_6^{2+}$ follow the Hückel's rule and proposed $C_6(SeH)_6^{2+}$, $C_6(TeH)_6^{2+}$, $C_6(SeH_2)_6^{2+}$ as viable candidates. In 2017, Rauhalahti et al. analyzed the ring currents of most of these structures.[11] Their GIMIC[16–18] calculations confirmed the existence of two concentric clockwise (diatropic) ring currents in $C_6I_6^{2+}$ and $C_6At_6^{2+}$, although the external current

density is approximately 50% weaker than that of the C_6-ring. More recently, Furukawa and coworkers studied the hexakis (phenylselenyl)benzene dication aromaticity.[19] These authors also determined, via X-ray diffraction, that the C—C bond lengths of the internal C_6-ring are practically identical to benzene.

These findings motivated us to examine the putative concentric σ- and π-delocalization in substituted benzene dications through the analysis of the induced magnetic field ($\mathbf{B}^{ind}$)[20,21] and its orbital contributions,[22] in order to provide a more detailed description of the electron delocalization and the role played by σ- and π-electrons. We consider all systems that presumably contain concentric ring currents, the dicationic substituted benzenes with formula $C_6R_6^{2+}$ (R=I, At, SeH, $SeCH_3$, TeH, $TeCH_3$). Our results show that both σ- and π-delocalized electrons produce an enhanced shielding region. However, while the internal carbon ring is shielded by the effects of strong diatropic currents caused by σ- and π-electrons, the external R_6-ring is strongly shielded but mainly by a σ-current. So, in general, these systems have a concentric aromatic character, whose carbon ring is doubly $(\sigma+\pi)$-delocalized and the external ring is just σ-delocalized. We also discuss why the strengths of the currents of the internal ring are more pronounced than those of the R_6-ring, and how in some cases, relativistic corrections affect their magnetic response, as in $C_6At_6^{2+}$.

1.1. Computational Methods

All geometries were fully optimized at the PW91/def2-TZVP level.[23,24] NMR computations were performed at the same level using the gauge-independent atomic orbital method (GIAO).[25,26] These computations were made in Gaussian 09.[27] The induced magnetic field, $\mathbf{B}^{ind}$ (a vector), was computed in two planes (a molecular and a transversal plane) employing planes of 10 Å per side (41 points per side), i.e., a total of 1681 points for each plane, using Aromagnetic,[28] placing the molecule on the xy-plane, the center of mass at the origin, and considering a uniform external field of 1T along the z-axis. Given this orientation, the z-component of $\mathbf{B}^{ind}$ (B^{ind}_z) is the

[a] M. Orozco-Ic, J. Barroso, Prof. G. Merino
Departamento de Física Aplicada
Centro de Investigación y de Estudios Avanzados
Unidad Mérida. Km 6 Antigua Carretera a Progreso. Apdo. Postal 73, Cordemex, 97310, Mérida, Yuc. (México)
E-mail: gmerino@cinvestav.mx
[b] Dr. R. Islas
Departamento de Ciencias Químicas
Facultad de Ciencias Exactas
Universidad Andres Bello
Av. República 275, 8320000 Santiago (Chile)

ChemistryOpen

Full Papers
doi.org/10.1002/open.202000105

Chemistry Europe
European Chemical
Societies Publishing

Figure 1. Profiles of $B^{ind}_z(z)$ of a) benzene, b) $(C_6H_6)^{2+}$, c) $C_6I_6^{2+}$, and d) $B-C_6(SeCH_3)_6^{2+}$ calculated at the PW91/def2-TZVP level.

largest one, so, the analysis of the magnetic response can be discussed in terms of this scalar field[20,21] via the visualization of isosurfaces, isolines, or profiles, as in NICS.[29,30] B^{ind}_z is given in µT units (equivalent to ppm), and its values are equal to $NICS_{zz}$ just for planar systems, as in the present cases.[15] The dissection of the shielding tensor into its canonical molecular orbital (CMO) contributions was performed employing the nuclear chemical shielding (NCS)[31] approach as is implemented in the NBO6 code.[32] For the case of rings of $C_6I_6^{2+}$ and $C_6At_6^{2+}$, B^{ind}_z was computed by introducing relativistic corrections and spin-orbit (SO) effects through the ZORA[33] approximation at the PW91/TZ2P level, using ADF2016.[34,35]

Table 1. B^{ind}_z values (ppm) computed at the center of the rings ($B^{ind}_z(0)$) at the PW91/def2-TZVP level.

Molecule	core	σ	π	Total
Benzene	−8.31	29.32	−36.41	−15.40
$(C_6H_6)^{2+}$	−8.18	−10.14	46.66	28.34
$C_6I_6^{2+}$	−6.82	−5.93	−26.13	−38.87
				−37.50[a]
	−7.47[b]	−10.13[b]	−22.28[b]	−39.90[b]
$C_6At_6^{2+}$				−46.10[a]
	−6.63[b]	−13.80[b]	−5.11[b]	−25.54[b]
$C_6(SeH)_6^{2+}$	−7.07	−2.21	−5.45	−14.73
$C_6(SeCH_3)_6^{2+}$	−8.51	−4.77	−19.59	−32.87
$B-C_6(SeCH_3)_6^{2+}$	−8.27	−2.88	−22.36	−33.51
$C_6(TeH)_6^{2+}$	−7.11	−19.82	−23.88	−50.81
$C_6(TeCH_3)_6^{2+}$	−9.27	−26.10	−13.77	−49.14

[a] Computed at the PW91/TZ2P and [b] at the SO-ZORA-PW91/TZ2P level.

2. Results and Discussions

Let us first analyze a typical $B^{ind}_z(z)$ profile of benzene. The $B^{ind}_z(z)$ profiles calculated for benzene along the z-axis are shown in Figure 1a. Specifically, $B^{ind}_z(0)$ is −15.40 ppm, of which core-, σ-, and π-electrons contribute with −8.31, 29.32, and −36.41 ppm, respectively (Table 1). So, core- and π-electrons produce a shielding response at the ring center. Notice that the core-contribution is not negligible at the ring center, but it rapidly tends to zero as z increases as the B^{ind}_z shows (Figure 1). It is mandatory to mention that the contribution from the core electrons computed using the NCS-GIAO[31] approach leads to larger values than those obtained through an ipsocentric method.[36,37] However, both formulations lead to similar total values and contributions from (core + σ)- and π-orbitals. Even though the core electrons produce a magnetic response, either large or small, this should not be taken into account for the discussion of aromaticity.[38] Concomitantly, the magnetic response of σ-electrons along the z-axis is positive and also vanishes to zero. This is not the case for the π-electrons because the corresponding profile has a minimum at z=0, and tends

slowly to zero. This shows that the π-electrons are responsible for the shielded cone in benzene,[21,22] but its σ-electrons induce a short-range deshielding region at the ring center and shielding regions located at the C−C bonds. This is the reason why aromaticity in benzene is discussed mostly in terms of the mobility of π-electrons.[39,40]

Let us now consider the B^{ind}_z profile of $C_6H_6^{2+}$. In the first place, the dicationic benzene is neither planar nor aromatic, as predicted by Hückel's rule.[41] The magnetic response along the z-axis is mainly induced by the π-electrons, but in contrast to benzene, it is positive, supporting an antiaromatic behavior and justifying the nonplanarity (see Table 1 and Figure 1b).

In $C_6I_6^{2+}$, the value of $B^{ind}_z(0)$ is −38.87 ppm, of which core-, σ-, and π-electrons and all negative and contribute with −6.82, −5.93, and −26.13 ppm, respectively (see Table 1). In other words, at the ring center, the σ-electrons contribute with 15.3 %. Note that at the ring center, the core electrons contribution (17.5 %) is even higher than the σ one. The B^{ind}_z profile indicates that the minimum for σ-electrons is not at the

ChemistryOpen

Full Papers
doi.org/10.1002/open.202000105

Chemistry Europe
European Chemical
Societies Publishing

ring center (Figure 1c), but at $z=1.5$ Å, suggesting that σ-electrons could induce a long-range shielding cone, certainly not in line with the benzene response! Clearly, profiles or single points computations of B^{ind}_z, NICS, or any variant can provide valuable information, but it is quite local, and some crucial details about the topology of these scalar fields might be lost. For instance, Hatanaka and coworkers dissected NICS(1) into the corresponding CMO contributions and found that the π-orbitals on C_6 (−12.5 ppm), the σ-orbitals localized on I (−6.2 ppm), and a mixture of σ- and core-orbitals on C_6 (−4.3 ppm), are responsible for the negative values at the ring center.[12] This conclusion is reinforced and clarified by analyzing the $C_6I_6^{2+}$ isolines (Figure 2). The response of all electrons promotes an intense shielding cone. The dissection of B^{ind}_z into its orbitals contributions shows that the π-electrons generate a shielding cone above (and below) the C_6-ring, as in the case of benzene,[21,22] but also in localized regions around the iodine atoms due to the p_z orbitals. Likewise, the σ- and core-electrons also produce a shielding region in both rings, but the σ-response is more intense.

Note that the σ-delocalization in $C_6I_6^{2+}$ is extended to the entire carbon ring (see Figure 2), something that it is not possible to recognize using one-point calculation. In other words, in contrast to benzene, $C_6I_6^{2+}$ exhibits an external σ-current that induces a shielding cone, reinforcing the delocalization in the carbon skeleton.[10] Specifically, the C—C bonds in benzene show shielded regions ranging between −45 and −50 ppm (see Figure S.1 in Supporting Information), while for $C_6I_6^{2+}$, they are more negative than −50 ppm (see Figure 2 and S.1). Conversely, the core-electrons are just effective in the
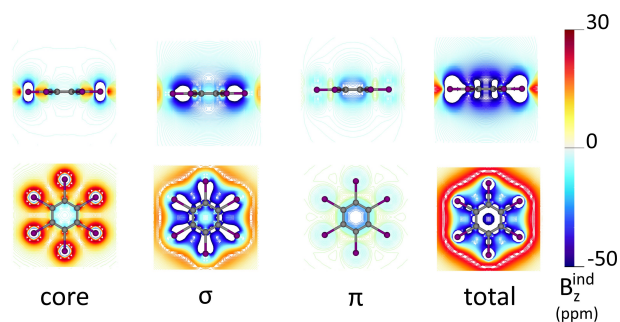
molecular plane and close to the nuclei. The long-range shielding effects on the C—I bonds and in the surroundings of iodine atoms are revealed by an even more pronounced shielding cone than that from π-electrons, indicating the flux of a strong diatropic σ-current in that area, in agreement with the topology of the reported ring current computations.[10,11] It is worth mentioning that these results do not occur with any other halogen as the substituent.[10,11]

For the case of $C_6(SeH)_6^{2+}$, the selected structure (the most energetically favorable) is characterized by an internal C_6-ring with an outer ring formed by SeH groups, where hydrogen atoms alternate above and below the molecular plane. The value of $B^{ind}_z(0)$ is −14.73 ppm (Table 1), with negative contributions from both σ- and π-electron, accounting for 15% and 37%, respectively. Notice that the largest contribution comes from the core electrons, with 48% of the total of $B^{ind}_z(0)$! Removing the core response, which in principle should be not viewed as responsible for aromaticity,[38] we can claim that the π-contribution is the one that contributes most to the total, but it is based on the information provided by just one point. However, the σ-profile of B^{ind}_z exhibits a shielded response reaching a minimum at 1.3 Å (−17.74 ppm, see Figure 3a). In contrast, the minimum of the π-profile is at the ring center and has values less negative than $C_6I_6^{2+}$ along the z-axis. This is also reflected in the B^{ind}_z isolines illustrated in Figure S.2. The small π-values are maintained around the molecular plane, and the shielding cone is barely noticeable while the σ-electrons govern the total magnetic behavior. Therefore, the π-delocalization in this system is not as strong as in the previous cases. Also, in this case, the core electrons contribute to short-shielding regions close to the nuclei.

The ring current analysis of the permethylated system $C_6(SeCH_3)_6^{2+}$, whose structure is similar to the $C_6(SeH)_6^{2+}$ case, was reported by Rauhalahti et al.[11] For this system, σ-electrons contribute 15% to the total $B^{ind}_z(0)$ of −32.87 ppm and π-electrons provide up to 60%. The $B^{ind}_z(z)$ profiles reveal that the shielded response along the z-axis is enhanced with respect to its hydrogen congener, reaching their minima (−22.05 ppm) for σ-electrons at around $z=1$ (see Figure 3b), and both σ- and π-responses are stronger than those of $C_6(SeH)_6^{2+}$. The existence of a shielding cone induced by the valence electrons and the evidence of $(\sigma+\pi)$-delocalization in the carbon ring is revealed through the visualization of the B^{ind}_z isolines (Figure 4). In fact, the σ-delocalization is the strongest one. So, a simple
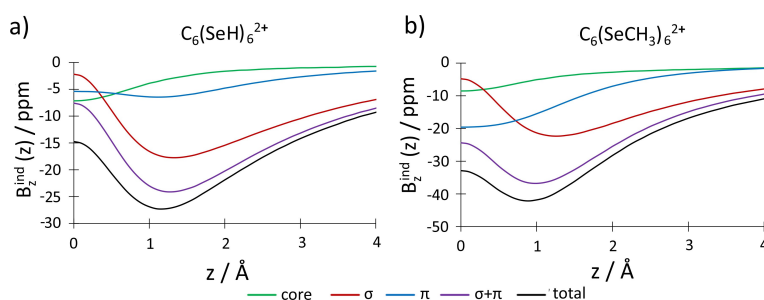

Figure 2. Isolines of $B^{ind}_z(z)$ for $C_6I_6^{2+}$ calculated at the PW91/def2-TZVP level. The negative (shielded) and positive (deshielded) values are illustrated in blue and red, respectively.

Figure 3. Profiles of $B^{ind}_z(z)$ of a) $C_6(SeH)_6^{2+}$ and b) $C_6(SeCH_3)_6^{2+}$ computed at the PW91/def2-TZVP level.

ChemistryOpen

Full Papers
doi.org/10.1002/open.202000105

**Chemistry
Europe**

European Chemical
Societies Publishing

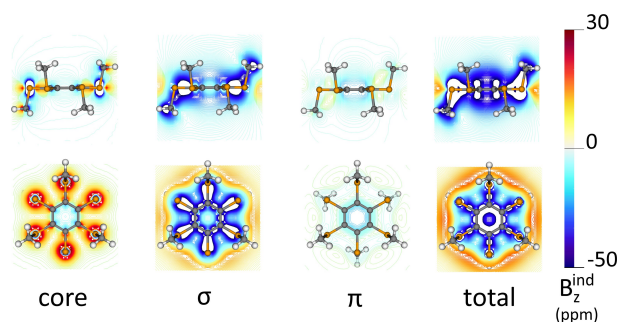**Figure 4.** Isolines of $B^{ind}_z(z)$ for $C_6(SeCH_3)_6^{2+}$ calculated at the PW91/def2-TZVP level. The negative (shielded) and positive (deshielded) values are illustrated in blue and red, respectively.

substitution of hydrogens in $C_6(SeH)_6^{2+}$ by methyl groups increases the magnetic response of both σ- and π-electrons, resulting in a very similar magnetic behavior of $C_6(SeCH_3)_6^{2+}$ to $C_6I_6^{2+}$, with a double and concentric aromatic character where the carbon ring is (σ+π)-shielded.

Furukawa et al.[19] analyzed a second isomer of $C_6(SeCH_3)_6^{2+}$, labeled by us as **B**-$C_6(SeCH_3)_6^{2+}$, with three adjacent methyl groups pointing above the plane and the rest pointing downward. Although this isomer is around 5 kcal/mol less stable than the Rauhalahti isomer, the position of its substituents matches that of the phenyl groups of the hexakis(phenylselenyl)benzene dication. The magnetic response for both isomers are quite similar over the entire space (see Figure 1d and S.3), enhancing the shielding response with respect to $C_6(SeH)_6^{2+}$ by a π-current in the C_6-ring and a stronger σ-current surrounding the Se-ring. However, the main contribution to the shielding response is caused by the σ-electrons of C−Se, which flow around both outer and C_6-ring with an intense diatropic current density, in line with the reported GIMIC computations,[11] so the reason why the current strength in the internal ring is higher than in the outer ring is that in the former, both σ- and π-electrons flow into carbon ring while in the external one, there are only delocalized σ-electrons (Figure S.3).[20] Therefore, we may assume a similar double delocalization in the carbon ring of the hexakis(phenylselenyl)benzene dication and a σ- one in the selenium ring.

For the case of the systems with tellurium, $C_6(TeH)_6^{2+}$ and $C_6(TeCH_3)_6^{2+}$, which have alternated hydrogens and methyl groups, respectively, the shielding response is notably superior to the Se compounds. Specifically, $C_6(TeH)_6^{2+}$ exhibits a total $B^{ind}_z(0)$ of −51.80 ppm, with contributions divided in 14%, 39%, and 47% for the core-, σ-, and π-electrons, respectively. As Figure S.4 shows, the σ-profile has a minimum of about −30 ppm while the core- and π-profile have their minimum at $z=0$. The B^{ind}_z isolines describe more appropriately this exceptional double shielding response (Figure S.5). In fact, they show a large shielding cone above the C−Te bonds, a sign that a strong diatropic σ-current is flowing in that region as previous ring current analysis showed.[11] This also explains why the carbon ring is strongly shielded because both σ- and π-electrons produce a shielding cone above the carbon ring. The case of $C_6(TeCH_3)_6^{2+}$ has a similar behavior, i.e., −9.27 (19%),

−26.10 (53%), and −13.77 (28%) ppm for the core-, σ-, and π-electrons of the total $B^{ind}_z(0)$ (−49.14 ppm), respectively. The shielded response by the σ- and π-electrons is also maintained at long-range, implying once more, a (σ+π)-delocalization in the carbon skeleton and a σ-shielded outer ring, as Figure S.6 illustrates.

Until this moment, we did not consider the contribution of relativistic and SO corrections in shielding tensor, which is well-known that could modify the numbers as the atomic number increases.[42] Rauhalahti et al.[11] computed the current strength for $C_6I_6^{2+}$, including the relativistic contributions, and found that this quantity differs by just 4% when relativistic corrections are considered via pseudopotentials. Let us analyze these contributions to B^{ind}_z in the heaviest systems, $C_6I_6^{2+}$ and $C_6At_6^{2+}$, along the z-axis. In our case, $C_6I_6^{2+}$ exhibits a $B^{ind}_z(0)$ value that differs by 1 ppm between non-relativistic (at the all electron PW91/TZ2P level) and relativistic calculations (at the all-electron SO-ZORA-PW91/TZ2P level), i.e., −37.50 and −39.90 ppm, respectively (Table 1). This small difference is maintained along the B^{ind}_z profile (see Figure S.7a). So, the relativistic effects on $C_6I_6^{2+}$ do not noticeably affect the numerical result for either in the ring current strength or B^{ind}_z values. The relativistic $B^{ind}_z(0)$ values for core-, σ-, and π-contributions are −7.47, −10.13, and −22.28 ppm, respectively. The B^{ind}_z profiles dissected in its orbitals contributions computed with relativistic corrections are depicted in Figure S.8. Although these profiles were performed with a different methodology than those in Figure 1a, the similarity is remarkable, and the computations at non-relativistic PW91/def2-TZVP level are reliable as well as it has been shown.

However, the case of $C_6At_6^{2+}$ is different. For the non-relativistic (at the PW91/TZ2P level), the $B^{ind}_z(0)$ value is −46.10 ppm. For the relativistic calculations computed at the SO-ZORA-PW91/TZ2P level, the total is −25.54 ppm (less negative than the non-relativistic value), where σ- and π-electrons represent 54% and 20%, respectively. The values of B^{ind}_z values along the z-axis differ considerably to those without the corrections (see Figure S.7b). Therefore, as astatine is a heavy element, relativistic and SO effects play a significant role and non-relativistic computations are unreliable. Likewise, the corrections must be considered in the whole magnetic response of $C_6At_6^{2+}$ and not just at one point, as the B^{ind}_z profiles shown in Figure S.9. Notice that the σ-response is strongly more shielded than in $C_6I_6^{2+}$ along the z-axis. That is, the σ-delocalization increases as does the atomic number of the substituent, whereas the π-contribution is reduced significantly with respect to the $C_6I_6^{2+}$. Note that for π-electrons, the minimum is close to 1 Å, while for σ-electrons is at 1.5 Å.

3. Conclusions

The induced magnetic field for the systems with formula $C_6R_6^{2+}$ (R=I, At, SeH, SeCH₃, TeH, TeCH₃) indicates that they are aromatic. The dissected analysis of the B^{ind}_z suggested evidence of concentric aromaticity. It is concentric in the sense that the internal carbon ring responds with strong shielding cones, which is caused by the three responses, i.e., the core-, σ-, and

ChemistryOpen

Full Papers
doi.org/10.1002/open.202000105

Chemistry Europe
European Chemical
Societies Publishing

π-electrons. Unlike benzene, the C_6-ring is $(\sigma + \pi)$-delocalized! Moreover, a σ-diatropic ring current flows around the external R_6-ring, indicating that the substitution of the benzene produces a double $(\sigma + \pi)$-delocalization in the carbon skeleton and a σ-delocalization in the external ring, which implies a stronger internal ring current. This behavior has not been found with any other substituted benzene. Furthermore, the spin-orbit and relativistic effects in the computation of the magnetic response, although not so relevant to $C_6I_6^{2+}$, are mandatory for $C_6At_6^{2+}$.

Acknowledgement

Conflict of Interest

The authors declare no conflict of interest.

[1] G. Merino, M. Solà, *Phys. Chem. Chem. Phys.* **2016**, *18*, 11587–11588.
[2] A. I. Boldyrev, L.-S. Wang, *Chem. Rev.* **2005**, *105*, 3716–3757.
[3] C. Liu, I. A. Popov, Z. Chen, A. I. Boldyrev, Z.-M. Sun, *Chem. Eur. J.* **2018**, *24*, 14583–14597.
[4] J. M. Mercero, A. I. Boldyrev, G. Merino, J. M. Ugalde, *Chem. Soc. Rev.* **2015**, *44*, 6519–6534.
[5] T. R. Galeev, A. I. Boldyrev, *Annu. Rep. Prog. Chem. Sect. C* **2011**, *107*, 124–147.
[6] A. P. Sergeeva, B. B. Averkiev, A. I. Boldyrev, *Metal-Metal Bonding* (Ed.: G. Parkin), Springer Berlin Heidelberg, Berlin, Heidelberg **2010**, pp. 275–305.
[7] X. Li, A. E. Kuznetsov, H.-F. Zhang, A. I. Boldyrev, L.-S. Wang, *Science* **2001**, *291*, 859–861.
[8] R. Islas, T. Heine, G. Merino, *J. Chem. Theory Comput.* **2007**, *3*, 775–781.
[9] D. J. Sagl, J. C. Martin, *J. Am. Chem. Soc.* **1988**, *110*, 5827–5833.
[10] R. W. A. Havenith, P. W. Fowler, S. Fias, P. Bultinck, *Tetrahedron Lett.* **2008**, *49*, 1421–1424.
[11] M. Rauhalahti, S. Taubert, D. Sundholm, V. Liégeois, *Phys. Chem. Chem. Phys.* **2017**, *19*, 7124–7131.
[12] M. Hatanaka, M. Saito, M. Fujita, K. Morokuma, *J. Org. Chem.* **2014**, *79*, 2640–2646.
[13] P. von R. Schleyer, C. Maerker, C. A. Dransfeld, H. Jiao, N. J. R. van Eikema Hommes, *J. Am. Chem. Soc.* **1996**, *118*, 6317–6318.
[14] Z. Chen, C. S. Wannere, C. Corminboeuf, R. Puchta, P. v R Schleyer, *Chem. Rev.* **2005**, *105*, 3842–3888.
[15] H. Fallah-Bagher-Shaidaei, C. S. Wannere, C. Corminboeuf, R. Puchta, P. v R Schleyer, *Org. Lett.* **2006**, *8*, 863–866.
[16] J. Jusélius, D. Sundholm, J. Gauss, *J. Chem. Phys.* **2004**, *121*, 3952–3963.
[17] H. Fliegl, S. Taubert, O. Lehtonen, D. Sundholm, *Phys. Chem. Chem. Phys.* **2011**, *13*, 20500–20518.
[18] D. Sundholm, H. Fliegl, R. J. F. Berger, *WIREs Comput. Mol. Sci.* **2016**, *6*, 639–678.
[19] S. Furukawa, M. Fujita, Y. Kanatomi, M. Minoura, M. Hatanaka, K. Morokuma, K. Ishimura, M. Saito, *Nat. Commun.* **2018**, *1*, 60.
[20] R. Islas, T. Heine, G. Merino, *Acc. Chem. Res.* **2012**, *45*, 215–228.
[21] G. Merino, T. Heine, G. Seifert, *Chem. Eur. J.* **2004**, *10*, 4367–4371.
[22] T. Heine, R. Islas, G. Merino, *J. Comput. Chem.* **2007**, *28*, 302–309.
[23] J. P. Perdew, J. A. Chevary, S. H. Vosko, K. A. Jackson, M. R. Pederson, D. J. Singh, C. Fiolhais, *Phys. Rev. B* **1992**, *46*, 6671–6687.
[24] F. Weigend, R. Ahlrichs, *Phys. Chem. Chem. Phys.* **2005**, *7*, 3297–3305.
[25] R. Ditchfield, *Mol. Phys.* **1974**, *27*, 789–807.
[26] K. Wolinski, J. F. Hinton, P. Pulay, *J. Am. Chem. Soc.* **1990**, *112*, 8251–8260.
[27] M. J. Frisch, G. W. Trucks, H. B. Schlegel, G. E. Scuseria, M. A. Robb, J. R. Cheeseman, G. Scalmani, V. Barone, B. Mennucci, G. A. Petersson, H. Nakatsuji, M. Caricato, X. Li, H. P. Hratchian, A. F. Izmaylov, J. Bloino, G. Zheng, J. L. Sonnenberg, M. Hada, M. Ehara, K. Toyota, R. Fukuda, J. Hasegawa, M. Ishida, T. Nakajima, Y. Honda, O. Kitao, H. Nakai, T. Vreven, J. J. A. Montgomery, J. E. Peralta, F. Ogliaro, M. Bearpark, J. J. Heyd, E. Brothers, K. N. Kudin, V. N. Staroverov, T. Keith, R. Kobayashi, J. Normand, K. Raghavachari, A. Rendell, J. C. Burant, S. S. Iyengar, J. Tomasi, M. Cossi, N. Rega, J. M. Millam, M. Klene, J. E. Knox, J. B. Cross, V. Bakken, C. Adamo, J. Jaramillo, R. Gomperts, R. E. Stratmann, O. Yazyev, A. J. Austin, R. Cammi, C. Pomelli, J. W. Ochterski, R. L. Martin, K. Morokuma, V. G. Zakrzewski, G. A. Voth, P. Salvador, J. J. Dannenberg, S. Dapprich, A. D. Daniels, O. Farkas, J. B. Foresman, J. V. Ortiz, J. Cioslowski, D. J. Fox, *Gaussian 09*, Revision C.01 ed., Gaussian Inc, Wallingford CT **2010**.
[28] M. Orozco, J. L. Cabellos, G. Merino, *Aromagnetic*, Cinvestav Mérida **2016**.
[29] J. O. C. Jiménez-Halla, E. Matito, J. Robles, M. Solà, *J. Organomet. Chem.* **2006**, *691*, 4359–4366.
[30] A. Stanger, *J. Org. Chem.* **2006**, *71*, 883–893.
[31] J. A. Bohmann, F. Weinhold, T. C. Farrar, *J. Chem. Phys.* **1997**, *107*, 1173–1184.
[32] E. D. Glendening, C. R. Landis, F. Weinhold, *J. Comput. Chem.* **2013**, *34*, 1429–1437.
[33] E. v Lenthe, A. Ehlers, E.-J. Baerends, *J. Chem. Phys.* **1999**, *110*, 8943–8953.
[34] G. te Velde, F. M. Bickelhaupt, E. J. Baerends, C. Fonseca Guerra, S. J. A. van Gisbergen, J. G. Snijders, T. Ziegler, *J. Comput. Chem.* **2001**, *22*, 931–967.
[35] T. Z. E. J. Baerends, A. J. Atkins, J. Autschbach, O. Baseggio, D. Bashford, A. Bérces, F. M. Bickelhaupt, C. Bo, P. M. Boerrigter, L. Cavallo, C. Daul, D. P. Chong, D. V. Chulhai, L. Deng, R. M. Dickson, J. M. Dieterich, D. E. Ellis, M. van Faassen, L. Fan, T. H. Fischer, A. Förster, C. Fonseca Guerra, M. Franchini, A. Ghysels, A. Giammona, S. J. A. van Gisbergen, A. Goez, A. W. Götz, J. A. Groeneveld, O. V. Gritsenko, M. Grüning, S. Gusarov, F. E. Harris, P. van den Hoek, Z. Hu, C. R. Jacob, H. Jacobsen, L. Jensen, L. Joubert, J. W. Kaminski, G. van Kessel, C. König, F. Kootstra, A. Kovalenko, M. V. Krykunov, E. van Lenthe, D. A. McCormack, A. Michalak, M. Mitoraj, S. M. Morton, J. Neugebauer, V. P. Nicu, L. Noodleman, V. P. Osinga, S. Patchkovskii, M. Pavanello, C. A. Peeples, P. H. T. Philipsen, D. Post, C. C. Pye, H. Ramanantoanina, P. Ramos, W. Ravenek, J. I. Rodríguez, P. Ros, R. Rüger, P. R. T. Schipper, D. Schlüns, H. van Schoot, G. Schreckenbach, J. S. Seldenthuis, M. Seth, J. G. Snijders, M. Solà, M. Stener, M. Swart, D. Swerhone, V. Tognetti, G. te Velde, P. Vernooijs, L. Versluis, L. Visscher, O. Visser, F. Wang, T. A. Wesolowski, E. M. van Wezenbeek, G. Wiesenekker, S. K. Wolff, T. K. Woo, A. L. Yakovlev, *ADF 2016*, SCM, Vrije Universiteit, Netherlands **2016**.
[36] E. Steiner, P. W. Fowler, *J. Phys. Chem. A* **2001**, *105*, 9553–9562.
[37] E. Steiner, P. W. Fowler, *Phys. Chem. Chem. Phys.* **2004**, *6*, 261–272.
[38] M. Orozco-Ic, J. Barroso, N. D. Charistos, A. Muñoz-Castro, G. Merino, *Chem. Eur. J.* **2020**, *26*, 326–330.
[39] J. Juselius, D. Sundholm, *Phys. Chem. Chem. Phys.* **1999**, *1*, 3429–3435.
[40] G. Monaco, R. Zanasi, *J. Phys. Chem. A* **2014**, *118*, 1673–1683.
[41] E. Hückel, *Z. Phys.* **1931**, *70*, 204–286.
[42] A. C. Castro, E. Osorio, J. O. C. Jiménez-Halla, E. Matito, W. Tiznado, G. Merino, *J. Chem. Theory Comput.* **2010**, *6*, 2701–2705.